Wearable Assistive Tactile Communication Interface Based on Integrated Touch Sensors and Actuators

Oliver Ozioko, Prakash Karipoth, Marion Hersh, and Ravinder Dahiya

***Abstract*— This paper presents the design and fabrication of a wearable tactile communication interface with vibrotactile feedback for assistive communication. The interface is based on finger Braille, which is a simple and efficient tactile communication method used by deafblind people. It consists of a flexible piezoresistive sensor and a vibrotactile actuator integrated together and positioned at the index, middle and ring fingers of both hands to represent the six dots of Braille. The sensors were made using flexible piezoresistive material whereas the actuator utilizes electromagnetic principle by means of a flexible coil and a tiny NdFeB permanent magnet. Both were integrated to realize a Bluetooth-enabled tactile communication glove which enables deafblind people to communicate using Braille codes. The evaluation with 20 end-users (10 deafblind and 10 sighted and hearing person) of the tactile interface under standardized conditions demonstrated that users can feel and distinguish the vibration at frequencies ranging from 10Hz to 200Hz which is within the perceivable frequency range for the FA-II receptors. The results show that it took non-experts in Braille within 25s and 55s to send and receive words like "BEST" and "JOURNAL", with an accuracy of ∼75% and 68% respectively.**

***Index Terms*— Actuator, deafblind communication, finger braille, tactile sensor, tactile display.**

I. Introduction

TACTILE communication is a vital aspect of social life and deafblind people heavily rely on this because they are unable to communicate via visual/auditory means [1]. In this regard, a tactile communication interface capable of providing touch feeling as well as the tactile feedback is much desired [2]. This also falls within the growing field of sensory substitution [3], where devices (e.g. tactile interfaces) are utilized to provide sensory information through some form of stimulation (vibration, heat, electrocutaneous) [4]. Tactile feedback is also needed in prosthetics [5], [6] and human-robot interaction, where eSkin like solutions are being developed to provide tactile feeling and haptic feedback [7]–[10]. Over the past decade, many devices have been developed for the purpose of sensory substitution for various assistive purposes [11], [12]. These devices utilize tactile sensors and actuators based on various technological approaches [13]–[15] and are based on different assistive technologies [1], [16], [17].

One of the popular tactile communication methods for deafblind people is the Braille. It is essentially a tactile method used for reading and writing by the blind and deafblind people [27], [28]. A Braille cell is made up of six dots, and the combinations of raised dots represent letters, numbers and special characters [29], [30]. By touching and exploring the Braille cell with fingertips the user identifies the raised dots and thereby interprets the characters. Typically, 100-300 separate cells per minute could be achieved for experienced users [31]. Various Braille-based devices reported for the blind and deafblind people, including Braille displays [28], [29], [32], [33], and body-braille devices [19] are compared in Table I. Considering the difficulty to learn and practice these conventional Braille methods [34], [35], finger Braille communication method, using the index, middle and ring fingers of both hands representing the six dots of Braille,

TABLE I
EXISTING ASSISTIVE TACTILE INTERFACES USING BRAILLE

Device	Tactile Sensor Used	Tactile Feedback Actuator Used	Year	Ref.
Portable Comm. Aid	None	None (Uses Braille Display)	2001	[18]
Body Braille	Braille Keypad	Microvibrators	2008	[19]
P-brll	Braille Keypad	Microvibrators	2012	[20]
Comm. Glove	Capacitive sensors	Vibration Motors	2015	[21]
SPARSHA	None (Braille keys)	Movable pins	2013	[22]
UbiBraille	None	Vibration Motors	2013	[23]
MyVox	None (uses Keyboard)	Braille Display/ Vibration Motor	2014	[24]
V-Braille	None (uses phone screen)	None (uses Mobile Phone Screen)	2010	[25]
SmartFinger Braille	Force Sensing Resistor	Vibration Motors	2017	[26]
This Work	Piezoresitive Sensor	Electromagnetic Vibrotactile Actuator	2020	

Manuscript received October 2, 2019; revised February 27, 2020; accepted March 29, 2020. Date of publication April 23, 2020; date of current version June 5, 2020. This work was supported in part by the Engineering and Physical Sciences Research Council (EPSRC) through Engineering Fellowship for Growth—PRINTSKIN under Grant EP/M002527/1, in part by the neu PRINTSKIN under Grant EP/R029644/1, and in part by the Tertiary Education and Trust Fund (TETFund) Nigeria, Deafblind Scotland, Sense Scotland, and Deafblind U.K. *(Corresponding author: Ravinder Dahiya.)*

Oliver Ozioko, Prakash Karipoth, and Ravinder Dahiya are with the Bendable Electronics and Sensing Technologies (BEST) Group, James Watt School of Engineering, University of Glasgow, Glasgow G12 8QQ, U.K. (e-mail: ravinder.dahiya@glasgow.ac.uk).

Marion Hersh is with the Department of Biomedical Engineering, James Watt School of Engineering, University of Glasgow, Glasgow G12 8QQ, U.K.

Digital Object Identifier 10.1109/TNSRE.2020.2986222

This work is licensed under a Creative Commons Attribution 4.0 License. For more information, see https://creativecommons.org/licenses/by/4.0/

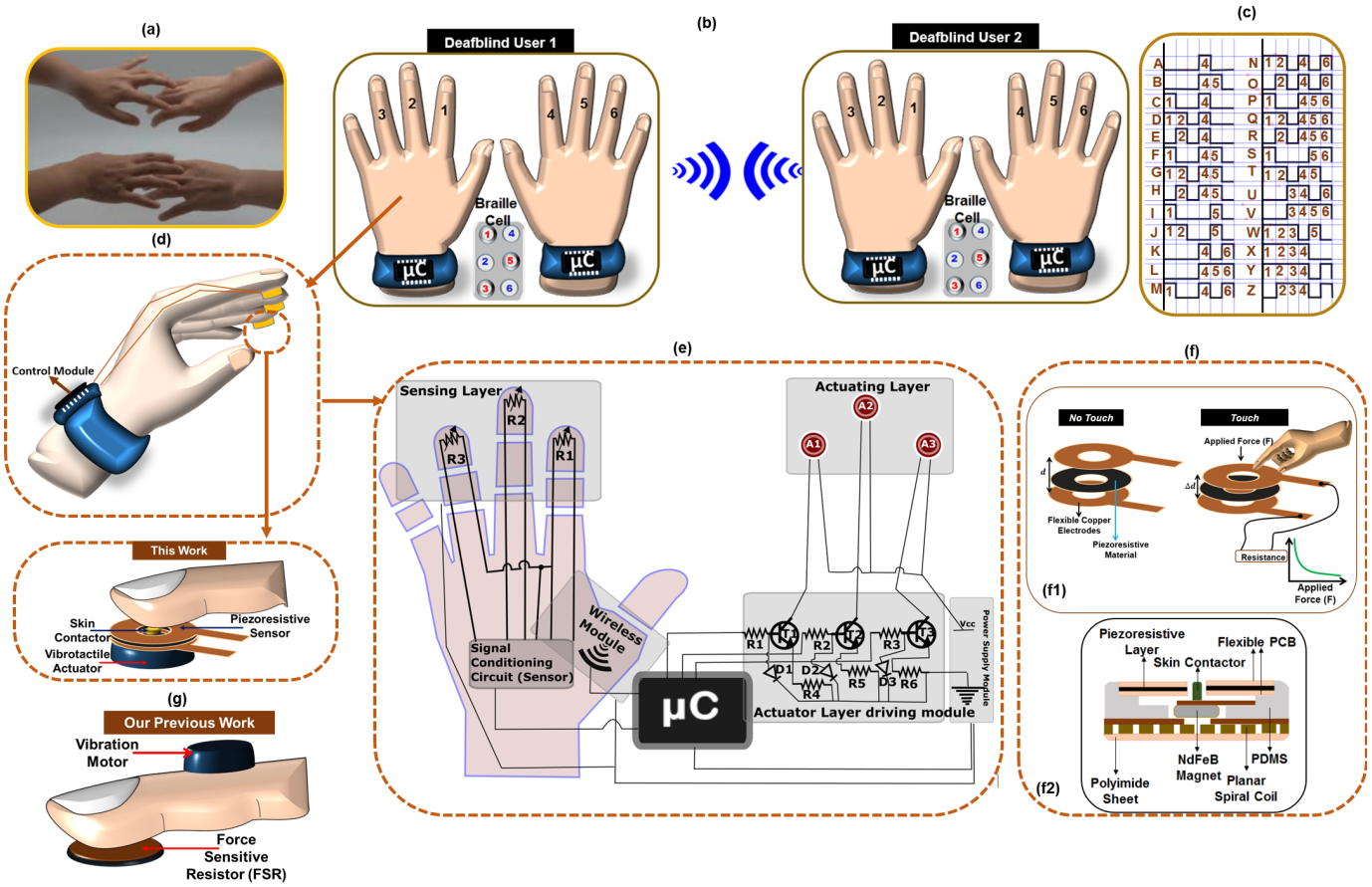

Fig. 1. (a) Tactile communication by deafblind people without tactile interface (b) Wireless tactile communication between two deafblind people using the tactile interface device; (c) Braille code (d) Schematic showing where sensors/actuators were attached (e) Functional block diagram of the interface; (f) The configuration and working principle of the sensing and actuation layer; (g) comparison with respect to previous work.

is being explored as an alternative [36]. Few finger Braille based solutions are also compared in Table I. This includes the mobile phone-based Braille devices which use a mobile app to recognize the voice of a normal person, displays it on the phone screen using an equivalent finger Braille code, and follows this code to sign on the corresponding fingers of the deafblind person [37]. However, such methods do not allow deafblind user to learn and operate independently. In this scenario, a communication glove with touch sensors and actuator can be more effective, as we demonstrated recently [26]. With commercial force sensing resistors (FSR) as touch sensors located at the tip of the index, middle and ring fingers and coin vibration motors on other side of the fingers of both hands (Fig.1g), this glove could provide the six dots of Braille code. However, from user feedbacks, we identified that this arrangement is still inconvenient due to limited wearability as the overall design is bulky, and the sensors and actuators remain disintegrated. The isolated location of sensors and actuators may bring difficulty for the deafblind while trying to interpret the messages. The innovative tactile communication interface presented here overcomes these issues, as also confirmed by the 20 users (10 deafblind and 10 normal) who could feel and distinguish the vibration at frequencies ranging from 10Hz to 200Hz. Normal finger braille-based communication by deafblind people (i.e. without a tactile interface) is by physically touching each other as shown in Fig. 1a. With the communication interface presented in this paper, the deafblind person will also be able to communicate remotely (Fig. 1b) using the integrated piezoresistive sensors and vibrotactile actuators. To achieve this, the wearable tactile interface is needed with touch sensors and vibrotactile actuator at the same point on the index, middle and ring fingers of both hands. This would enable the device to send and receive messages on the same location using finger Braille method. The device presented here addresses this requirement and comprises of a flexible piezoresistive sensor integrated with a flexible electromagnetic coil-based actuator positioned at the index, middle and ring fingers of both hands to represent the six dots of Braille (Fig. 1b).

This paper is organized as follows: Section II presents the structure of the device and its operating principle. Section III describes the fabrication of the individual components of the device and their integration as single device. Section IV presents the characterization of the tactile interface and its components; and in Section V, user participation and feedback is presented. Finally, the conclusion of the work is summarized in Section VI.

II. Description of the Tactile Interface

Fig. 1 shows the concept of finger braille communication system and the structure of the piezoresistive sensors and actuators used for the tactile interface along with their

operating principle. The finger braille tactile communication interface presented here consists of three main modules; (1) the sensing-actuation module; (2) wireless module; and (3) the control module. The sensing-actuator module is made up of two layers – a piezoresistive sensing layer (Fig. 1(f1)) and an electromagnetic vibrotactile actuating layer (Fig. 1(f2)). Each piezoresistive sensor is tightly integrated with a vibrotactile actuator to enable two-way communication via touch sensing and vibrotactile feedback at same location on the tip of user's fingers (Fig. 1d). The drive circuit for the sensors and actuators was built around an ATmega32U4 microcontroller with 12 analogue inputs, 16 MHz crystal oscillator, 20 digital I/O pins in which 7 can be used as PWM outputs (Fig. 1e). This controls both the sensing and actuating layer as functionally shown in Fig. 1(e) and the wireless communication was realized using Bluetooth module. The actuator module is driven using a constant current source built using bipolar junction transistors. The signal conditioning circuit for the sensor is realized using a voltage divider read via the10-bit analog to digital converter (ADC) of the microcontroller. The index, middle and ring fingers of both left and right hands contain the integrated piezoresistive sensor and vibrotactile actuator at the fingertips for two-way communication (Fig. 1b). While the sensing part is used for sending messages, the vibrotactile actuator is used to provide vibrotactile feedback.

To communicate, the user taps the enabled fingers on any hard surface in a specific sequential combination that corresponds to the Braille code (Fig. 1c) which is then processed and decoded by the control module shown in Fig. 1(e). The decoded code is transmitted to a nearby or distant user via Bluetooth. When messages are received, the corresponding vibrotactile actuator(s) on the receiver's hand vibrates to interpret the incoming message accordingly.

Fig. 1(d) shows the typical design of the interface, containing a tandem of the piezoresistive pressure sensors and vibrotactile actuators on the fingertips. Fig. 1(f) shows the structure of the piezoresistive sensing layer, which consists of two conducting copper electrodes (fabricated using flexible printed circuit board (FPCB)) with a piezoresistive material sandwiched between them. When a normal external pressure is applied on the surface of the sensor, the electrical resistance of the material proportionally decreases. This change in resistance is quantified and used to sense the applied pressure. Fig. 1(f1) shows the configuration and working principle of the actuator module. It uses electromagnetic principle and hence works via the magnetic field interaction of a spiral coil and a permanent magnet. When a pulsating current is applied on the coil, at a set frequency, a proportional magnetic field is generated along the axis of the coil as shown in Fig. 1(f). The generated pulsating magnetic field interacts with an integrated permanent magnet to create actuation and hence vibration.

III. Fabrication of the Tactile Interface

A. Fabrication of the Piezoresistive Tactile Sensor

As described in the previous Section (Fig.1f) the sensor consists of a piezoresistive material (velostat – polymer impregnated with carbon black from Adafruit) with volume resistivity

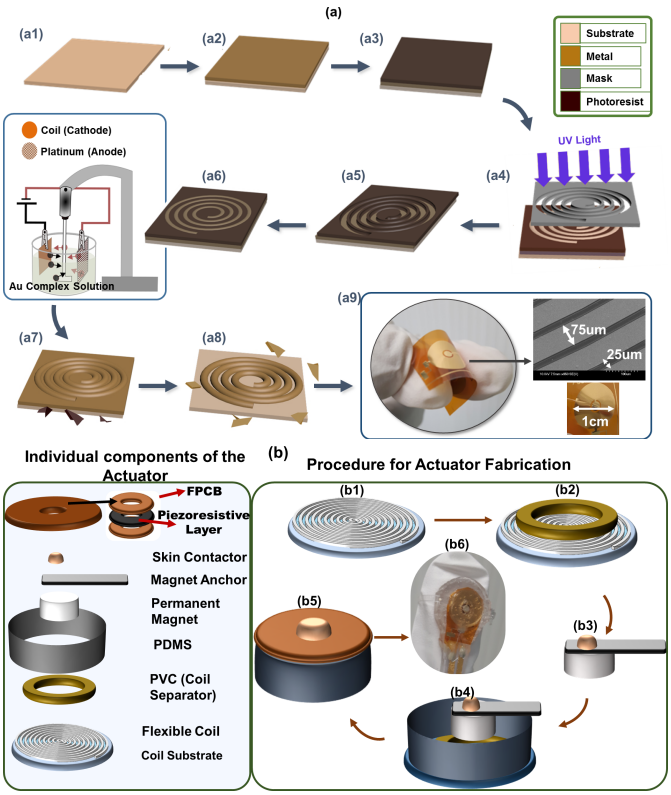

Fig. 2. (a) Fabrication Scheme for the spiral coil of vibrotactile actuator (a1) Initial flexible substrate; (a2) Gold deposition; (a3) Spin-coating of photoresist; (a4) Exposure of photoresist; (a5) Developing the photoresist; (a6) Electroplating the coil; (a7) lift-off the photoresist; (a8) Etching of the seed layer; (a9) Fabricated coil (b) Procedure for the realization of the touch-sensitive vibrotactile actuator.

<500 ohm-cm, and surface Resistivity <31,000 ohm/ cm^2 sandwiched between two FPCBs used as top and bottom electrode.

A CAD model of electrodes with 1cm outer diameter and 0.3cm inner diameter was used for patterning of both FPCBs and piezoresistive material using the Silhouette Cameo software. The FPCB was then bonded to the sticky 12 x 12 cutting mat of the Silhoutte Cameo 2 in readiness for cutting. The speed, force, and blade position of the blade cutter were set to 5, 20, and 10 $cm.s^{-1}$ respectively to selectively cut through the required layer only. Afterwards, the piezoresistive material was sandwiched between the patterned FPCB and electrical contacts were made with the top and bottom electrodes.

B. Fabrication of the Vibrotactile Actuation Module

Fig. 2 shows the steps followed for the fabrication of the vibrotactile actuator [38]. The spiral coil was fabricated by adopting the LIGA (Lithographie Galvanoformung Abformung) process (Fig. 2a) which is used to realize structures with up to 1mm thickness [39]. This method was considered to realize a relatively thicker coil for higher magnetic field strength. The first step is the deposition of a 20nm/50nm NiCr/Au layer on a 50 μm polyimide sheet using Plassys MEB 550S Electron Beam Evaporator system. This is followed by the spinning of AZ4562 photoresist on the polyimide sheet at a

speed of 2000 rpm for 3 seconds. Afterwards, the sample was left at room temperature for about 30 minutes to allow some solvent to evaporate which is necessary to avoid bubbles being trapped within the photoresist. Following this, the sample was baked at 100 °C on a hotplate for 10 minutes. The sample is again left in ambient air for 30 minutes before exposing it to ultraviolet (UV) for 60 minutes following standard lithography technique. The next is the development of the exposed photoresist using AZ826 developer for 10 minutes and rinsing in reverse osmosis water.

The sample is then gold-plated by connecting the sample to the cathode of a non-cyanide gold complex electroplating solution for ∼42 minutes to achieve a ∼16 μm thick coil with 45 turns. The choice of non-cyanide gold plating solution is because of its non-toxicity, high plating efficiency, compatibility with photoresists, and controllable residual stress of the plated gold [40]. The unwanted gold layer was then etched using a gold etchant for ∼14 seconds exposing the NiCr seed layer. Following this, the sample was annealed at 350 °C in a furnace for ∼20 minutes under Nitrogen ambient. This is a necessary step the failure of which may lead to the undesirable lift-off of the entire coil pattern. The final step is the etching of the NiCr seed layer using Nichrome etchant. This process exposes only the plated ∼16 μm spiral coil pattern on the substrate (Fig. 2).

Fig. 2b shows the steps followed to realize the electromagnetic actuator for integration with touch sensing layer. The individual components used for the fabrication of the actuator include the piezoresistive touch-sensitive layer, the coil, a PVC-based coil separator, a permanent magnet, magnet anchor, skin contactor; all assembled together and packaged using PDMS.

The actuator has an overall diameter of 1.5 cm selectively designed to fit appropriately at the fingertip providing maximum convenience to the user. In a typical fabrication procedure, a cylindrical mould with 1.5cm, 2cm and 0.3cm as inner diameter, outer diameter and the height respectively was utilized to realize a PDMS packaging of diameter 1.5cm and height 0.3cm. In order to obtain the PDMS body, a PDMS mixture comprising of Sylgard 184 pre-polymer base and crosslinking agent was prepared in the ratio 10:1 and poured into the mould and then cured at 80°C in the oven for 12 minutes.

The fully integrated actuator is now realized by careful assembly of different components. First, the coil separator (PVC) was attached to the coil substrate using Loctite transparent adhesive and then the moulded PDMS soft body of the actuator was also attached on top of the coil substrate. Then a 2mm thick N42 grade Neodymium magnet purchased from E-Magnets was tethered to the PDMS packaging in a cantilever-like structure using the magnet anchor made using PVC (Fig. 2(b3) & (b4)). A 1mm diameter skin contactor made of Polylactic acid (PLA) plastic was attached to the permanent magnet using Loctite transparent adhesive. Finally, piezoresistive touch-sensitive layer is also attached and was designed to cover up the remaining space within the PDMS body. The sensor in tandem with the vibrotactile actuator were integrated into a glove realized using flexible

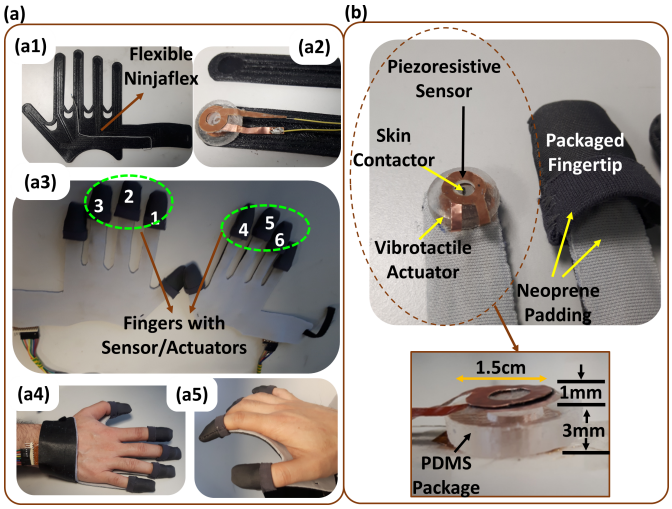

Fig. 3. (a) Glove layout before integrating the devices (b) Layout with integrated device before covering (c) Packaged fingertip (d) Glove showing flexibility (e) Entire glove (f) Back of the glove (g) Zoomed in fingertip (h) Single device and its dimension.

3D printed material ninjaflex (yield strength 4MPa, melting point of 216°C) as the base and neoprene fabric as an overlay for comfort (Fig. 3).

IV. Characterization

The device characterization was carried out in three parts, as the characterization of: (1) piezoresistive sensing layer; (2) vibrotactile actuator; and, (3) tactile communication interface. These are explained below.

A. Characterization of the Piezoresistive Sensing Layer

In order to independently characterize the performance of the fabricated piezoresistive sensors, each of them was firmly attached to a stable 1004 aluminum single point low-capacity load cell which can measure the force applied on the sensor via a square glass probe. The load cell yields 1.5mV for every 1N of applied force and was connected to an E4980AL LCR meter which measures the change in resistance. Pulses of 5N force were then applied on the sensor using the square glass probe and the resistance variations were automatically recorded via the LabVIEW program.

Fig. 4(a) shows the fabricated flexible touch sensing layer before its integration with the actuating layer. Fig. 4(a) shows the resistance variation for different applied forces (0 to 10N) for all the six sensors. The error bars in Fig. 4(a) show the standard deviation for the six sensors fabricated and this ranges from 3.8% to 15.5%. For repeatability, the coefficient of variance was also computed and this ranges from 13% up to 50%. Although this is higher than 10% variation recommended for clinical applications [41], it could be suitable for finger Braille application where force level is not mapped to critical treatment conditions.

Further, this is also within the repeatability of 15% reported by Sensitronics ThruMode™ for their single-point force sensitive resistor (Sensitronics, Bow, WA, USA). Fig. 4(b) and (c) show the result of characterizing the sensor with 5N force at

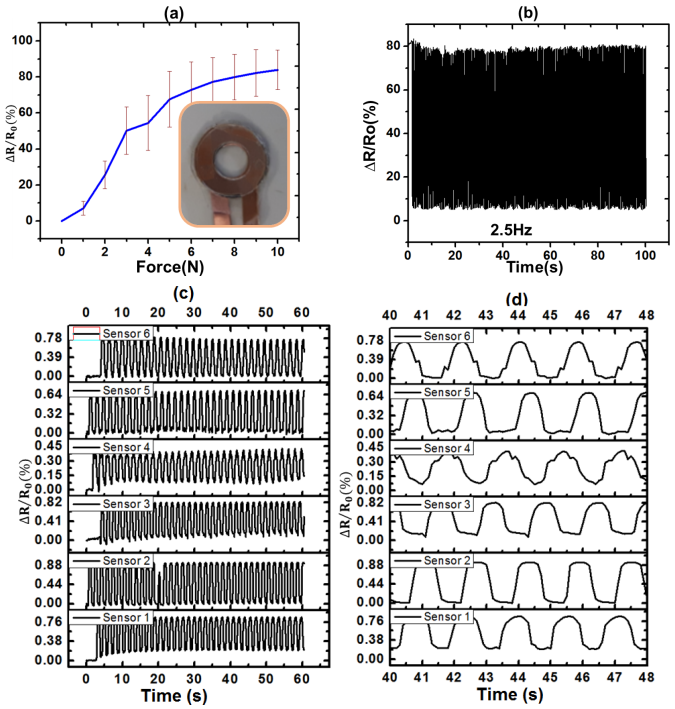

Fig. 4. (a) Force-resistance characteristics (0 to 10N) for the six sensors (b) Cyclic loading of the piezoresistive pressure sensors using 5N at 2.5Hz; (c) Cyclic loading of the piezoresistive pressure sensors using 5N at 0.625Hz (d) zoom-in of the cyclic loading between 40 and 49 seconds.

2.5Hz and all the six sensing layers at 0.625Hz respectively. Evidently, the sensors showed good stability and reasonable average relative change in resistance ($\Delta R/Ro$ up to $\sim$75%). The sensors equally showed an average response time of 0.36s and a recovery time of 0.24s. An average Braille user reads less than 100 cells per minute (>0.6s for 1 cell) [31] and so 0.6s for both response and recovery time could be suitable for sensors used in the finger Braille application [31]. The typical hysteresis behavior in piezoresistive sensors is negligibly evident in all the sensors. However, the sensors experienced some drift and consequently all the sensors could not return perfectly to the baseline when unloaded.

B. Characterization of the Vibrotactile Actuation Layer

Fig. 5 shows the characterization result for vibrotactile actuator. This was carried out by following the optical lever technique. This is a reliable approach for magnifying and measuring the small dynamic or static displacement using optical technique. In this method, a flat mirror or any reflecting surface is fixed on the device whose displacement is to be measured. A low power laser ray is directed at a suitable angle from a source to the mirror on the device and the reflection of the ray is projected on to a screen forming a spot. When the device actuates, the laser spot on the screen is also displaced synchronously from its equilibrium position. By properly measuring and calibrating the position and displacement of the spot, the exact amplitude of actuation of the device can be estimated using image processing techniques implemented in MATLAB. In our experiment, a custom-made optical lever was used. It consists of a pointed laser source, a reflective mirror on the top of the actuator, a white screen and a high-speed camera which can record at 960 frames per second (fps). To drive

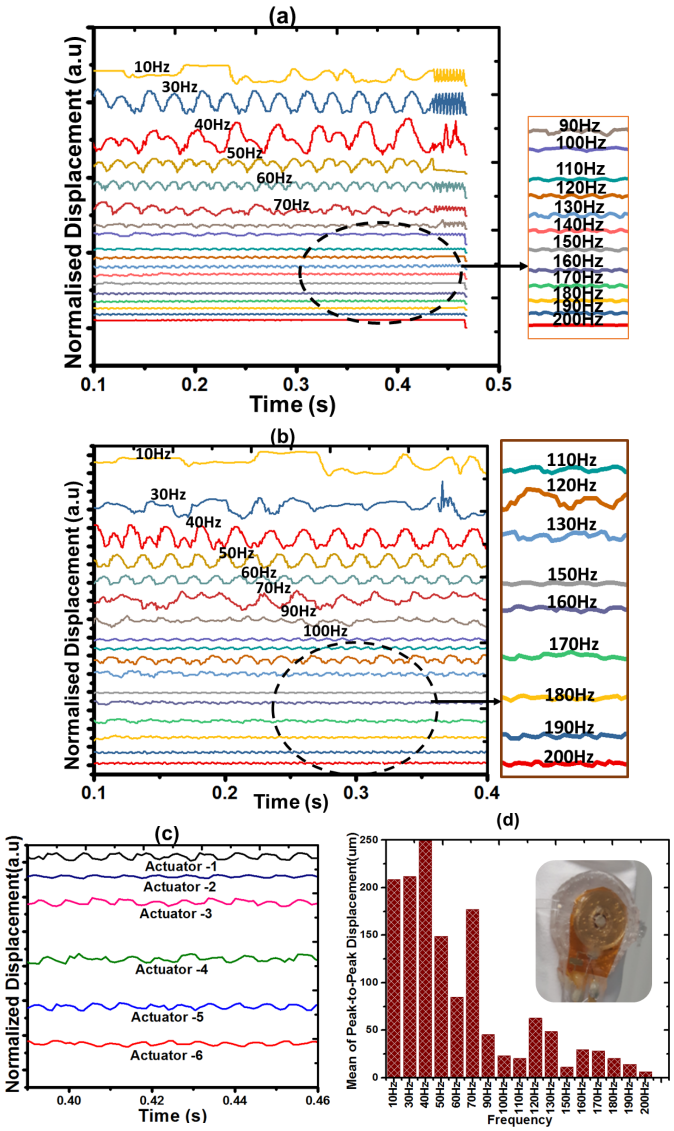

Fig. 5. (a) Normalized displacement of an actuator at 30mA for frequencies ranging from 10 to 200Hz; (b) Normalized displacement of an actuator at 150mA for frequencies ranging from 10 to 200Hz; (c) Normalized displacement of six different actuators at 150mA and 150Hz; (d) Mean peak-to-peak displacement of the six actuators.

the actuator, a signal generator, power supply and a simple constant current drive circuit was employed.

Prior to measurements, the pointed laser was directed onto the reflective mirror on top of the actuator and adjusted properly to obtain a sharp spot on the screen. The camera was also focused accurately to ensure that it captures the spot properly and the setup was left undisturbed throughout the experiment. During the experiment, the actuator was driven using a uniform square pulse of current at different frequencies ranging from 10Hz to 200Hz which is chosen to fall within the frequency range of the FA-II of the human hand [42]. This produced a pulsating magnetic field of corresponding frequency along the axis of the coil. The produced magnetic field exerts a periodic magnetic impulsive force on the tiny magnet of the actuator which causes a corresponding displacement and hence vibration of the actuator. The displacement was observed at a higher magnitude as an oscillatory displacement of the laser spot on the screen. The motion of the laser spot during the

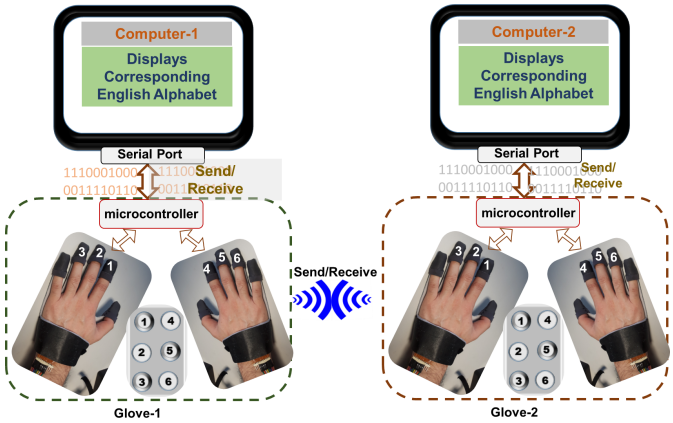

Fig. 6. Scheme used for characterization of the tactile communication interface.

vibration of the actuator was recorded with the high-speed camera at a frame rate of 960fps.

Fig. 5 shows the normalized displacement of the actuator at 30mA and 150mA respectively for the frequency range of 10Hz to 200Hz. At 10Hz the moving magnet undergoes higher damping which causes random oscillatory behavior before coming to its rest position. In most cases (especially at frequencies <90Hz (Fig 5a and b), the actuators did not get sufficient time to restore to its equilibrium state before the succeeding input current pulse, resulting in some shift from its steady state. This pulse may cause constructive or destructive interference with the damped oscillation. Considering the mean peak-to-peak displacement (Fig. 5(d)), the resonant frequency of the actuator is around 40Hz which is enough to stimulate the Pacinian Corpuscle of the human skin [42]. The increase in actuator displacement at some other frequencies could be attributed to frequency overtone (e.g. at 120Hz, 160Hz and 190Hz). Generally, higher displacement of the actuators occurred at lower frequencies with maximum displacement ($\sim$191μm) observed at 40Hz. Fig. 5c shows the normalized displacement of the six actuators with an average displacement of 5 μm at 150Hz and 150mA.

C. Characterization of the Tactile Communication Interface

Following the characterization of the sensors and actuators, the finger braille tactile communication interface was characterized, as shown in Fig. 6. The glove was interfaced with a computer and used to communicate via Bluetooth with a testing glove similar to the one we presented in [26]. The communication protocol allows two deafblind users to communicate via Bluetooth wireless. Each interface is able to interpret the braille communication logic. The output of each glove is displayed on a computer using the serial monitor of Arduino software. Braille codes for all letters from A to Z were tapped on the glove and in each case the corresponding letter displayed on the computer screen is recorded. This was done 14 times for each letter and in each case, the number of times the letter was displayed correctly as well as incorrectly was recorded. This was analyzed by computing a confusion matrix as shown in Fig. 7. It shows that only letters A and B were

ACTUAL \ PREDICTED	A	B	C	D	E	F	G	H	I	J	K	L	M	N	O	P	Q	R	S	T	U	V	W	X	Y	Z	Total
A	14	0	0	0	0	0	0	0	0	0	0	0	0	0	0	0	0	0	0	0	0	0	0	0	0	0	14
B	0	14	0	0	0	0	0	0	0	0	0	0	0	0	0	0	0	0	0	0	0	0	0	0	0	0	14
C	2	0	12	0	0	0	0	0	0	0	0	0	0	0	0	0	0	0	0	0	0	0	0	0	0	0	14
D	3	0	2	9	0	0	0	0	0	0	0	0	0	0	0	0	0	0	0	0	0	0	0	0	0	0	14
E	3	0	0	0	11	0	0	0	0	0	0	0	0	0	0	0	0	0	0	0	0	0	0	0	0	0	14
F	1	0	0	0	0	13	0	0	0	0	0	0	0	0	0	0	0	0	0	0	0	0	0	0	0	0	14
G	0	0	0	0	0	1	13	0	0	0	0	0	0	0	0	0	0	0	0	0	0	0	0	0	0	0	14
H	0	0	0	0	0	0	1	13	0	0	0	0	0	0	0	0	0	0	0	0	0	0	0	0	0	0	14
I	0	0	0	0	1	0	0	0	13	0	0	0	0	0	0	0	0	0	0	0	0	0	0	0	0	0	14
J	0	0	0	0	0	0	0	0	1	13	0	0	0	0	0	0	0	0	0	0	0	0	0	0	0	0	14
K	0	0	0	0	0	0	0	0	0	0	14	0	0	0	0	0	0	0	0	0	0	0	0	0	0	0	14
L	0	0	0	0	0	0	0	0	0	0	2	12	0	0	0	0	0	0	0	0	0	0	0	0	0	0	14
M	0	0	0	0	0	0	0	0	0	0	0	1	13	0	0	0	0	0	0	0	0	0	0	0	0	0	14
N	0	0	0	0	0	0	0	0	0	0	0	0	1	13	0	0	0	0	0	0	0	0	0	0	0	0	14
O	0	0	0	0	0	0	0	0	0	0	0	0	0	0	12	2	0	0	0	0	0	0	0	0	0	0	14
P	0	0	3	0	0	0	0	0	0	0	0	0	0	0	0	11	0	0	0	0	0	0	0	0	0	0	14
Q	0	0	0	0	0	0	0	0	0	0	0	0	0	0	0	0	4	10	0	0	0	0	0	0	0	0	14
R	0	0	0	0	0	0	0	0	0	0	0	0	0	0	0	0	0	7	7	0	0	0	0	0	0	0	14
S	0	0	0	0	0	0	0	0	0	0	0	0	0	0	0	0	0	0	1	13	0	0	0	0	0	0	14
T	0	0	0	0	0	0	0	0	0	0	0	0	0	0	0	0	0	0	2	12	0	0	0	0	0	0	14
U	0	0	0	0	0	0	0	0	0	0	0	0	0	0	0	0	0	0	0	6	8	0	0	0	0	0	14
V	0	0	0	0	0	0	0	0	0	0	0	0	0	0	0	0	0	0	0	0	4	10	0	0	0	0	14
W	0	0	0	0	0	0	0	0	0	0	0	0	0	0	0	0	0	0	0	0	0	2	12	0	0	0	14
X	0	0	0	0	0	0	0	0	0	0	0	1	0	0	0	0	0	0	0	0	0	0	2	11	0	0	14
Y	0	0	0	0	0	0	0	0	0	0	0	0	3	0	0	0	0	0	0	0	0	0	0	1	10	0	14
Z	0	0	0	0	0	0	0	0	0	0	1	0	0	0	1	0	0	0	0	0	0	0	0	0	2	10	14
Total	23	14	17	9	12	14	14	13	14	13	17	13	15	16	13	17	17	8	15	18	12	12	14	12	12	10	364

Fig. 7. Confusion matrix showing the performance of the Finger Braille Communication system.

decoded correctly 100% of the time, while the least accurate is letter R with 50% accuracy. For up to 7 different times, letter R was interpreted as Q which is 50% false positive. This could be attributed to the closeness of the Braille codes for both letters, some delay in sensor response and the user's comfortability in using the corresponding fingers. Generally, when letters were consciously repeated, they were interpreted correctly. The duration it takes from sending to reception of messages were also characterized and we observed it takes $\sim$25 seconds duration to send and receive the word B,E,S,T and 55 seconds for the word J,O,U,R,N,A,L. This demonstrated speed of communication is based on the skills of non-experts in Braille and so the efficiency could be improved with adaptive learning, given that most of the time was spent to mentally process which finger combination to tap.

V. User Participation and Feedback

Prior to user validation experiment, ethical approval was obtained from University of Glasgow ethics committee. During the user experiment, two partners wearing these touch-sensitive actuators on their fingers were guided to communicate by tapping a combination of the fingers on the desk to compose messages based on Braille code.

During the user evaluation, 20 users (10 deafblind People and 10 sighted and hearing people) were recruited in order to understand how the concept of the tactile interface meets their needs. A group of 10 deafblind users (aged between 25-60) were involved with the help of Deafblind Scotland, Sense Scotland and Deafblind UK. Another group of 10 non-disabled persons including guide communicators as well as others who are not associated with deafblind people were also involved in the study. These organizations were consulted in their official capacity, first through email and then visits to their offices. In general, the user experiment could be broadly classified into three parts: (1) Tactile perception test, carried out to understand how the vibration created by the actuator is perceived by the users at different frequencies; (2) Device communication evaluation, carried out to understand if the device is able to communicate wirelessly using the finger braille concept.

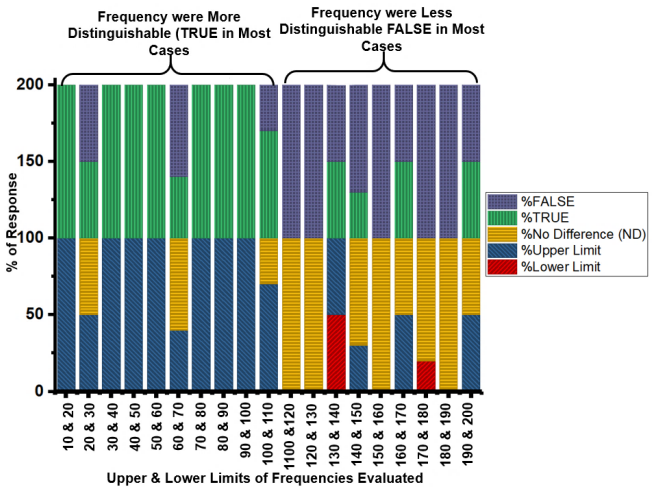

Fig. 8. Summary of the response obtained during the tactile perception test carried out with 10 deafblind and 10 non-disabled people.

(3) User feedback about the tactile communication interface: This was carried out primarily to obtain some user-centered feedback about the fabricated tactile interface.

A. Tactile Perception Test

Fig. 8 presents a summary of the results obtained during the tactile perception test carried out with 10 deafblind and 10 non-disabled people. It may be noted that the deafblind people are expected to have more sensitive fingertips than normal sighted and hearing people due to their developed tactile sensitivity [43], hence there is need to understand how they perceive the vibration produced by the fabricated interface. During this experiment, deafblind people were requested to touch and feel the vibration on the device and provide feedback whether the vibration is insufficient, enough or in excess. Sighted and hearing people also participated in this research by wearing ear plug and blind fold to mimic deafblind experience.

During the experiment, the actuator was excited at different frequencies ranging from 10 to 200Hz using a pulsating current of 150mA. These frequencies are in the same range over which the actuators were characterized (Fig. 5). At every instance, there is a lower and upper limit frequency, participants were asked to compare the vibration presented to them (at upper limit frequency) with the previous one (at lower limit frequency) and state which one is stronger, whether they are the same or if there were no difference (ND). In each case, the participants were not given any prior information about frequency being used. Where the user's response matches the actual scenario, it was recorded as TRUE; otherwise it was recorded as FALSE. It is evident from Fig. 5 that the actuator is capable of giving distinguishable vibrotactile feedback at frequencies ranging from 10 to 200Hz with more pronounced at lower frequencies (<100Hz). This shows a close match with the actuator characterization presented in Fig. 5, where variation in the amplitude of vibration was more distinguishable at lower frequencies (<100Hz). However, most users considered frequencies around 60Hz and 70Hz more convenient.

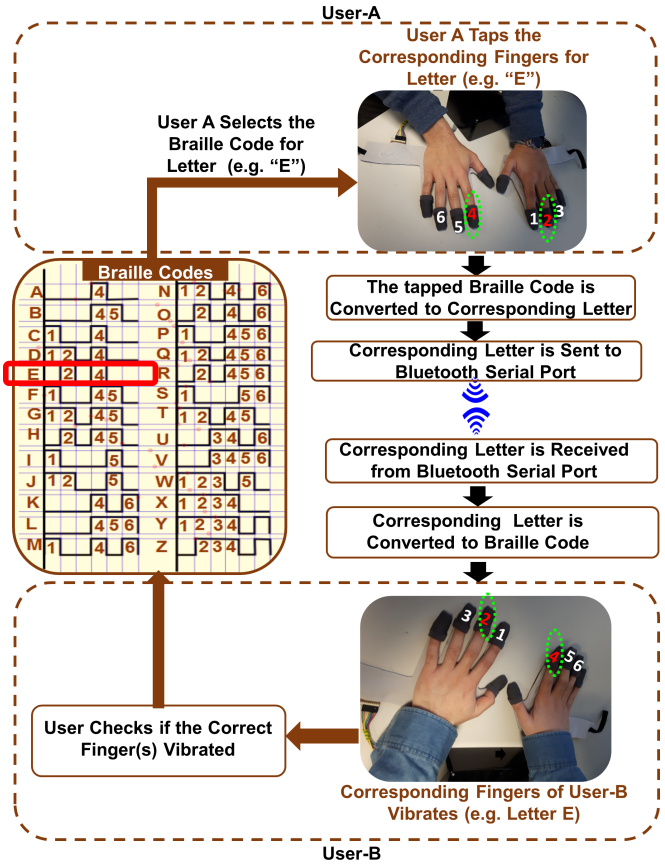

Fig. 9. Communication protocol between the users (A and B) during evaluation (using Letter "E" as example.

B. Device Communication Evaluation

Fig. 9 shows the scheme used during the communication evaluation and only eight of the recruited users participated in this test. This test involves glove-to-glove communication as opposed to the characterization in Section IV(C) and hence no computer was involved. English alphabets (e.g. letter "E") were sent from user A to B following the method shown in Fig. 9. The communication was carried out using the tactile interface similar to the "SmartFingerBraille" presented in [26]. One participant (User A) wore the touch-sensitive actuator presented in this work, while the other (User B) wore the SmartFingerBraille. User A was requested to tap a combination of the fingers on the glove corresponding to a Braille code. Specifically, letters B,E,S,T and J,O,U,R,N,A,L were typed (by tapping a combination of the fingers on a desk) and sent from user A to user B. Participants were generally told the corresponding fingers which were expected to vibrate upon the reception of each letter to maintain uniformity. Fig. 10 shows the result of sending these words using the glove. All vibration patterns were in accordance with the received messages. So, if a user sends the wrong braille code by tapping wrong fingers, the wrong fingers of the receiver (user B) vibrated. An average of ~75% accuracy was recorded for the word "BEST" and ~68% for the word "JOURNAL". Highest letter accuracy was recorded for B (88% for word "BEST") and U (88% for the word "JOURNAL"). Our observation is that the ability of the letters to be correctly interpreted depends

ACTUAL \ PREDICTED	A	B	C	D	E	F	G	H	I	J	K	L	M	N	O	P	Q	R	S	T	U	V	W	X	Y	Z	TOTAL
B	1	7	0	0	0	0	0	0	0	0	0	0	0	0	0	0	0	0	0	0	0	0	0	0	0	0	8
E	1	1	0	0	6	0	0	0	0	0	0	0	0	0	0	0	0	0	0	0	0	0	0	0	0	0	8
S	0	0	0	0	0	0	0	0	0	0	0	0	0	0	0	0	0	2	6	0	0	0	0	0	0	0	8
T	0	0	0	0	0	0	0	0	0	0	0	0	0	0	0	0	0	1	2	5	0	0	0	0	0	0	8
TOTAL	2	8	0	0	6	0	0	0	0	0	0	0	0	0	0	0	0	3	8	5	0	0	0	0	0	0	32
J	0	0	0	0	2	0	0	0	0	6	0	0	0	0	0	0	0	0	0	0	0	0	0	0	0	0	8
O	0	0	0	0	0	0	0	0	0	0	1	0	0	1	5	1	0	0	0	0	0	0	0	0	0	0	8
U	0	0	0	0	0	0	0	0	0	0	1	0	0	0	0	0	0	0	0	7	0	0	0	0	0	0	8
R	0	0	0	0	0	0	0	0	0	0	0	1	0	0	0	0	2	5	0	0	0	0	0	0	0	0	8
N	0	0	0	0	0	0	0	0	0	0	0	0	1	4	3	0	0	0	0	0	0	0	0	0	0	0	8
A	6	0	0	0	0	0	0	0	0	0	1	1	0	0	0	0	0	0	0	0	0	0	0	0	0	0	8
L	0	0	0	0	0	0	0	0	0	0	3	5	0	0	0	0	0	0	0	0	0	0	0	0	0	0	8
TOTAL	6	0	0	0	2	0	0	0	0	6	6	7	1	5	8	1	2	5	0	0	7	0	0	0	0	0	56

Fig. 10. Confusion matrix showing the performance of the communication interface when the word "BEST" and "JOURNAL" were communicated.

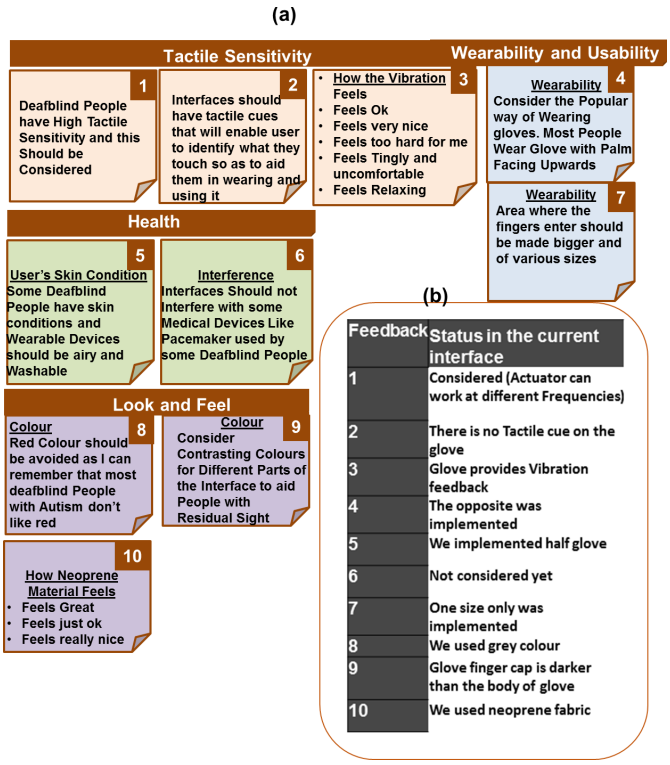

Fig. 11. Affinity diagram showing the feedback from users (in direct speech) for the user requirement interview carried out for the development of assistive tactile communication interface for deafblind people (b) Status of some feedback implemented already in this work.

on user's experience with using the device. This means that the reported accuracy could be improved with users who have experience in using braille.

C. Overall User Feedback on the Tactile Interface

Fig. 11 shows the qualitative results (in direct speech) of the feedback given by deafblind people about the fabricated interface with suggestions for improvements. The details of this interview are presented in the form of affinity diagram showing the themes and relationship between the responses of the participants. A semi-structured interview took place to understand the opinion of the participants regarding the device. Through this, the user opinion about the fabricated tactile interface was gathered and thematic analysis used to analyze the result as presented in Fig. 11.

Prior to the interview, an information sheet and consent form were distributed to the participants to help them understand various aspects involved in the experiment. The test was carried out on different days and with prime consideration was the availability and convenience for each participant. For the interview with deafblind people, we visited the organization during their meetings and had a one-on-one interaction with each. During the interview, the information was read and conveyed to the 10 deafblind participants by their interpreters and guide communicators. Sighted and hearing participants also read the information sheet and gave their consent. A brief introduction and guidance regarding the device design and its operation was also given to all these participants. Following this, the participants were requested to touch and wear the interface and then their feedback about the wearability and feel of the design were recorded. Suggestions were also sought from them regarding other aspects and features which could be improved or included for a more acceptable user experience.

VI. Conclusion

In this paper a novel tactile two-way communication interface based on finger braille was realized. The tactile interface consists of a tandem piezoresistive sensing and actuator module. Six such devices were fabricated and integrated to realize a tactile communication interface for deafblind people based on the concept of finger Braille. The sensors fabricated for this purpose showed maximum stability at 2.5Hz cyclic loading, whereas the actuator can provide uniform vibrations with input signals of frequencies ranging from 10Hz to 200Hz. Maximum amplitude of vibration was observed for 40Hz with 150mA which is within the perceivable frequency of the human Pacinian corpuscle. The user tests conclude that the deafblind users find the interface convenient to wear and use. Majority of the participants felt that frequencies around 60Hz and 70Hz provides comparatively more convenient perception of vibration. An average accuracy of ∼75% (within ∼25s duration from sending to receiving) was recorded for sending the word "BEST" and 68% (within ∼55s duration from sending to receiving) for the word "JOURNAL". This accuracy shall improve as the user gets used to the device and users were able to interpret the Braille codes sent through the tactile interface in the form of vibrations at specific fingers. This will enable the deafblind people who use Braille to easily communicate and will encourage non-Braille users to learn Braille. Further improvements in features such as durability, wearability and adoption of some of the user-requirement feedback (Fig. 11) are necessary for implementation in practical scale.

References

[1] F. Sorgini, R. Caliò, M. C. Carrozza, and C. M. Oddo, "Haptic-assistive technologies for audition and vision sensory disabilities," *Disab. Rehabil., Assistive Technol.*, vol. 13, no. 4, pp. 394–421, May 2018.
[2] S. Luo, J. Bimbo, R. Dahiya, and H. Liu, "Robotic tactile perception of object properties: A review," *Mechatronics*, vol. 48, pp. 54–67, Dec. 2017.
[3] P. Bach-Y-Rita, "Tactile sensory substitution studies," *Ann. New York Acad. Sci.*, vol. 1013, no. 1, pp. 83–91, 2004.
[4] L. Cancar, A. Díaz, A. Barrientos, D. Travieso, and D. M. Jacobs, "Tactile-sight: A sensory substitution device based on distance-related vibrotactile flow," *Int. J. Adv. Robotic Syst.*, vol. 10, no. 6, p. 272, Jun. 2013.

[5] D. J. Weber, M. Hao, M. A. Urbin, C. Schoenewald, and N. Lan, "Sensory information feedback for neural prostheses," in *Biomedical Information Technology*, D. D. Feng, Ed., 2nd ed. New York, NY, USA: Academic, 2020, pp. 687–715.

[6] E. D'Anna *et al.*, "A closed-loop hand prosthesis with simultaneous intraneural tactile and position feedback," *Sci. Robot.*, vol. 4, no. 27, Feb. 2019, Art. no. eaau8892.

[7] W. Navaraj and R. Dahiya, "Fingerprint-enhanced capacitive-piezoelectric flexible sensing skin to discriminate static and dynamic tactile stimuli," *Adv. Intell. Syst.*, vol. 1, no. 7, Nov. 2019, Art. no. 1900051.

[8] Y. Ling *et al.*, "Embedding pinhole vertical gold nanowire electronic skins for braille recognition," *Small*, vol. 15, no. 13, Mar. 2019, Art. no. 1804853.

[9] A. Polishchuk, W. T. Navaraj, H. Heidari, and R. Dahiya, "Multisensory smart glove for tactile feedback in prosthetic hand," *Procedia Eng.*, vol. 168, pp. 1605–1608, 2016.

[10] R. Dahiya *et al.*, "Large-area soft e-skin: The challenges beyond sensor designs," *Proc. IEEE*, vol. 107, no. 10, pp. 2016–2033, Oct. 2019.

[11] D. Dakopoulos and N. G. Bourbakis, "Wearable obstacle avoidance electronic travel aids for blind: A survey," *IEEE Trans. Syst., Man, Cybern. C, Appl. Rev.*, vol. 40, no. 1, pp. 25–35, Jan. 2010.

[12] S. K. Nagel, C. Carl, T. Kringe, R. Märtin, and P. König, "Beyond sensory substitution-learning the sixth sense," *J. Neural Eng.*, vol. 2, no. 4, p. R13, 2005.

[13] N. Yogeswaran *et al.*, "Piezoelectric graphene field effect transistor pressure sensors for tactile sensing," *Appl. Phys. Lett.*, vol. 113, no. 1, Jul. 2018, Art. no. 014102.

[14] W. Taube Navaraj *et al.*, "Nanowire FET based neural element for robotic tactile sensing skin," *Frontiers Neurosci.*, vol. 11, p. 501, Sep. 2017.

[15] A. Vilouras, H. Heidari, W. T. Navaraj, and R. Dahiya, "At-home computer-aided myoelectric training system for wrist prosthesis," in *Haptics: Perception, Devices, Control, and Applications* (Lecture Notes in Computer Science), vol. 9775, F. Bello, H. Kajimoto, and Y. Visell, Eds. Cham, Switzerland: Springer, 2016.

[16] W. T. Navaraj, H. Nassar, and R. Dahiya, "Prosthetic hand with biomimetic tactile sensing and force feedback," in *Proc. IEEE Int. Symp. Circuits Syst. (ISCAS)*, May 2019, pp. 1–4.

[17] O. Ozioko, M. Hersh, and R. Dahiya, "Inductance-based flexible pressure sensor for assistive gloves," in *Proc. IEEE SENSORS*, Oct. 2018, pp. 1–4.

[18] M.-C. Su, C.-Y. Chen, C.-H. Chou, Y.-C. Wang, S.-Y. Su, and H.-F. Hsiu, "Portable communication aid for deaf-blind people," *Comput. Control Eng. J.*, vol. 12, no. 1, pp. 37–43, Feb. 2001.

[19] S. Ohtsuka, N. Sasaki, S. Hasegawa, and T. Harakawa, "The introduction of tele-support system for deaf-blind people using body-braille and a mobile phone," in *Proc. 5th IEEE Consum. Commun. Netw. Conf.*, Las Vegas, NV, USA, Jan. 2008, pp. 1263–1264.

[20] S. Ohtsuka, N. Sasaki, S. Hasegawa, and T. Harakawa, "Helen keller Phone—A communication system for deaf-blind people using body-braille and skype," in *Proc. IEEE Consum. Commun. Netw. Conf. (CCNC)*, Jan. 2012, pp. 30–31.

[21] T. Choudhary, S. Kulkarni, and P. Reddy, "A braille-based mobile communication and translation glove for deaf-blind people," in *Proc. Int. Conf. Pervas. Comput. (ICPC)*, Jan. 2015, pp. 1–4.

[22] R. Sarkar, S. Das, and S. Roy, "SPARSHA: A low cost refreshable braille for deaf-blind people for communication with deaf-blind and non-disabled persons," in *Distributed Computing and Internet Technology*. Berlin, Germany: Springer, 2013, pp. 465–475.

[23] H. Nicolau, J. Guerreiro, T. Guerreiro, and L. Carriço, "UbiBraille: Designing and evaluating a vibrotactile braille-reading device," in *Proc. 15th Int. ACM SIGACCESS Conf. Comput. Accessibility (ASSETS)*, Bellevue, WA, USA, 2013, pp. 1–8.

[24] F. Ramirez-Garibay, C. Millan Olivarria, A. F. Eufracio Aguilera, and J. C. Huegel, "MyVox-device for the communication between people: Blind, deaf, deaf-blind and unimpaired," in *Proc. IEEE Global Humanitarian Technol. Conf. (GHTC)*, Oct. 2014, pp. 506–510.

[25] C. Jayant, C. Acuario, W. Johnson, J. Hollier, and R. Ladner, "V-braille: Haptic braille perception using a touch-screen and vibration on mobile phones," in *Proc. 12th Int. ACM SIGACCESS Conf. Comput. Accessibility (ASSETS)*, Orlando, FL, USA, 2010, pp. 295–296.

[26] O. Ozioko, W. Taube, M. Hersh, and R. Dahiya, "SmartFingerBraille: A tactile sensing and actuation based communication glove for deafblind people," in *Proc. IEEE 26th Int. Symp. Ind. Electron. (ISIE)*, Jun. 2017, pp. 2014–2018.

[27] A. Alfadhel, M. A. Khan, S. Cardoso de Freitas, and J. Kosel, "Magnetic tactile sensor for braille reading," *IEEE Sensors J.*, vol. 16, no. 24, pp. 8700–8705, Dec. 2016.

[28] A. Russomanno, S. O'Modhrain, R. B. Gillespie, and M. W. M. Rodger, "Refreshing refreshable braille displays," *IEEE Trans. Haptics*, vol. 8, no. 3, pp. 287–297, Jul. 2015.

[29] K. Fukuda *et al.*, "A 4 V operation, flexible braille display using organic transistors, carbon nanotube actuators, and organic static random-access memory," *Adv. Funct. Mater.*, vol. 21, no. 21, pp. 4019–4027, 2011.

[30] H.-J. Kwon, S. W. Lee, and S. S. Lee, "Braille dot display module with a PDMS membrane driven by a thermopneumatic actuator," *Sens. Actuators A, Phys.*, vol. 154, no. 2, pp. 238–246, Sep. 2009.

[31] W. Schiff and E. Foulke, *Tactual Perception: A Sourcebook*. Cambridge, U.K.: Cambridge Univ. Press, 1982.

[32] S. G. Lu *et al.*, "Large displacement in relaxor ferroelectric terpolymer blend derived actuators using al electrode for braille displays," *Sci. Rep.*, vol. 5, no. 1, p. 11361, Sep. 2015.

[33] Y. Kato *et al.*, "Sheet-type braille displays by integrating organic field-effect transistors and polymeric actuators," *IEEE Trans. Electron Devices*, vol. 54, no. 2, pp. 202–209, Feb. 2007.

[34] M. Hersh and S. Mouroutsou, "Learning technology and disability—Overcoming barriers to inclusion: Evidence from a multicountry study," *British J. Educ. Tech.*, vol. 50, no. 6, pp. 3329–3344, 2019.

[35] V. S. Morash, A. Russomanno, R. B. Gillespie, and S. O'Modhrain, "Evaluating approaches to rendering braille text on a high-density pin display," *IEEE Trans. Haptics*, vol. 11, no. 3, pp. 476–481, Jul. 2018.

[36] Y. Matsuda, I. Sakuma, Y. Jimbo, E. Kobayashi, T. Arafune, and T. Isomura, "Finger braille recognition system for non-disabled people who communicate with deafblind people," in *World Congress on Medical Physics and Biomedical Engineering*. Berlin, Germany: Springer, 2006, pp. 2935–2938.

[37] Y. Matsuda, I. Sakuma, Y. Jimbo, E. Kobayashi, T. Arafune, and T. Isomura, "Finger braille recognition system for people who communicate with deafblind people," in *Proc. IEEE Int. Conf. Mechatronics Autom.*, Aug. 2008, pp. 268–273.

[38] T. Kawasetsu, T. Horii, H. Ishihara, and M. Asada, "Flexible tri-axis tactile sensor using spiral inductor and magnetorheological elastomer," *IEEE Sensors J.*, vol. 18, no. 14, pp. 5834–5841, Jul. 2018.

[39] O. Brand, G. K. Fedder, and C. Hierold, *LIGA and its Applications*. Hoboken, NJ, USA: Wiley, 2009.

[40] M. Schlesinger and M. Paunovic, *Modern Electroplating*. Hoboken, NJ, USA: Wiley, 2011.

[41] S. Parmar, I. Khodasevych, and O. Troynikov, "Evaluation of flexible force sensors for pressure monitoring in treatment of chronic venous disorders," *Sensors*, vol. 17, no. 8, p. 1923, 2017.

[42] B. T. Nghiem *et al.*, "Providing a sense of touch to prosthetic hands," *Plastic Reconstructive Surgery*, vol. 135, no. 6, pp. 1652–1663, Jun. 2015.

[43] R. W. Van Boven, R. H. Hamilton, T. Kauffman, J. P. Keenan, and A. Pascual-Leone, "Tactile spatial resolution in blind Braille readers," *Neurology*, vol. 54, no. 12, pp. 2230–2236, 2000.